POROSITY AND SURFACE MORPHOLOGY OF LEAD SELENIDE – TIN SELENIDE LAYERS ON SILICON SUBSTRATES: X-RAY DIFFRACTION STUDIES

A.I. Mamontov [1], A.P. Petrakov [2], S.P. Zimin[3]

[1]Vyatka State Humanities University, Kirov, Russian Federation;

[2]Syktyvkar State University Named after Pitirim Sorokin, Syktyvkar, Russian Federation;

[3]P.G. Demidov Yaroslavl State University, Yaroslavl, Russian Federation

In the paper, the surface porosity and morphology of $Pb_{0.97}Sn_{0.03}Se$ films on silicon substrates subjected to anodic electrochemical etching in the Tompkins-Johnson's electrolyte at a current density of 1 mA/cm^2 have been studied using X-ray reflectometry. To reduce the difference in lattice parameters of a growing film, buffer CaF_2 layer (about 2 nm thick) and buffer PbSe one (about 400 nm thick) were used. The averaged thickness of re-precipitated near-surface selenium layer was determined to be 45 nm. The X-ray experimental results showed qualitative agreement with electron-microscopical data. It was established by high-resolution X-ray diffraction methods that macroporous structure with transverse and longitudinal porous projections of sizes 47 and 82 nm (relatively) was forming in electrochemical etching. The angle of porous tilt with the surface normal was found to be 34.5 degrees. The applicability of high-resolution X-ray methods to nondestructive investigation of porous structure was shown.

Key words: anodizing; porosity; total external reflection method; electrochemical etching; lead-tin selenide

Citation: A.I. Mamontov, A.P. Petrakov, S.P. Zimin, Porosity and surface morphology of lead selenide – tin selenide layers on silicon substrates: X-ray diffraction studies, St. Petersburg Polytechnical State University Journal. Physics and Mathematics. 11 (1) (2018) 67 – 74. DOI: 10.18721/JPM.11110

Introduction

Porous semiconductor materials now attract a great deal of attention due to their unique properties and potential applications. The processes of pore formation are actively studied in elemental semiconductors (silicon and germanium), in binary and ternary materials A^3B^5, A^2B^6 [1 – 3, etc.]. Lead chalcogenides (PbTe, PbSe, PbS and solid solutions based on them) that belong to the group of narrow-band semiconductors A^4B^6 are traditionally widely used in thermoelectric devices, optoelectronics devices of the IR range, solar cells, etc. Pore formation in these materials can lead to effective modification of structural, electrical and optical properties [4 – 7, etc.]. At the same time, it is extremely important to obtain data on the surface morphology, the structure of porous objects, the size of the pores and the magnitude of porosity. For example, it was established in [7] that the processes of pore formation in lead selenide and tin selenide films are accompanied by a significant reprecipitation of selenium on the walls of pores and on the surface.

The goal of this study has been to determine the pore and surface parameters of porous $Pb_{0.97}Sn_{0.03}Se$ films on silicon substrates using high-resolution X-ray methods. The presented results continue the studies published in [7].

Experimental procedure

Film samples of $Pb_{0.97}Sn_{0.03}Se/PbSe/CaF_2/Si(111)$ with a total thickness of 4.5 μm were grown by molecular beam epitaxy on a single-crystal Si(111) substrate. The size of the sub-

strate's mosaic blocks, determined by high-resolution X-ray diffraction [8], was approximately 30 μm. Thin buffer layers of CaF_2 (about 2 nm thick) and PbSe (about 400 nm) were used to reduce the discrepancy between the lattice parameter of the growing film (a_1 = 0.615 nm) and of the substrate (a_2 = 0.543 nm), as well as to reduce mechanical stresses in the ternary solid solution.

Pore formation in the near-surface layer of lead selenide – tin selenide was carried out in a vertical electrochemical cell with a platinum upper cathode at a current density of 1 mA/cm^2 for 10 min. The etching was done in the Tompkins and Johnson solution: 40 ml of glycerin, 10 ml of HNO_3, 10 ml of glacial acetic acid. The technology and basic properties of the porous structure of the obtained samples are described in [7].

High-resolution X-ray diffractometry and X-ray reflectometry studies were carried out using a DRON-UM1 X-ray powder diffractometer. The radiation of Cu$K_{\alpha 1}$ ($\lambda K_{\alpha 1}$ = 1.5405 Å, $\lambda K_{\alpha 2}$ = 1.5443 Å) was formed by a slit monochromator made of single-crystal silicon with a triple reflection (111) and vertical and horizontal collimator exit slits with the width of 2.0 mm and 0.1 mm, respectively.

The diffraction scheme was assembled with a goniometer allowing to register the angular deviation in three-crystal geometry with an accuracy of 0.1 arcsec. (Fig. 1, *a*). A planar Si(111) crystal analyzer was placed between the sample and the detector.

Data on the properties of the samples and their surfaces were obtained from the dependence of the detected intensity on the rotation angles of the sample and the analyzer. The method makes it possible to determine the interplanar spacings of epitaxial structures, as well as the pore parameters in porous materials. Scattering by a rough surface or scattering caused by defects can be separated from scattering by a perfect crystal.

The method of X-ray reflectometry, based on measuring the reflectivity of X-ray radiation in the angular region of total external reflection (TER), was also used in the study. A slit with the width S_2 = 0.25mm was placed in front of the detector for reflectometry measurements (Fig. 1, *b*).

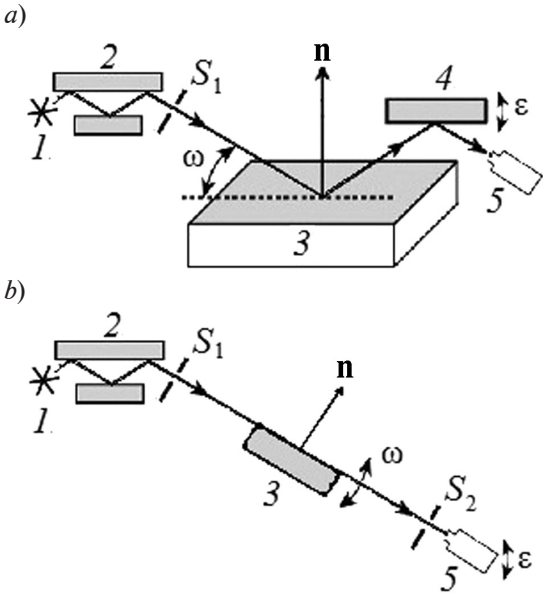

Fig. 1. Three-crystal diffraction (*a*) and reflectometric (*b*) schemes of X-ray imaging methods:
source of X-ray radiation *1*, monochromator *2*, sample *3*, analyzer *4*, detector *5*; **n** is the normal to the surface; S_1, S_2 are the slits; the notations for the angles are explained in the text

Processing and discussion of the results

The structural features of porous layers of $Pb_{0.97}Sn_{0.03}Se$ were studied by high-resolution three-crystal X-ray diffractometry (TCXRD). For this purpose, contours of equal diffuse scattering intensity were plotted on the X-ray patterns taken by the analyzer in scanning mode at different positions of the sample crystal [9]. The contours of equal intensity (Fig. 2) were constructed in inverse space according to the formulae:

$$q_z = (2\pi\varepsilon \cdot \cos\theta_B) / \lambda, \quad (1)$$

$$q_x = [2\pi(2\omega - \varepsilon)\sin\theta_B] / \lambda, \quad (2)$$

where ε and ω are, respectively, the angles by which the analyzer and the sample deviate from the Bragg angle; θ_B is the Bragg angle; λ is the X-ray wavelength.

The system had the following resolution: $\Delta q_z = 0.1(\mu m)^{-1}$, $\Delta q_x = 0.2(\mu m)^{-1}$.

Sufficiently perfect crystals are typically obtained through growing layers of lead selenide – tin selenide by molecular-beam epitaxy.

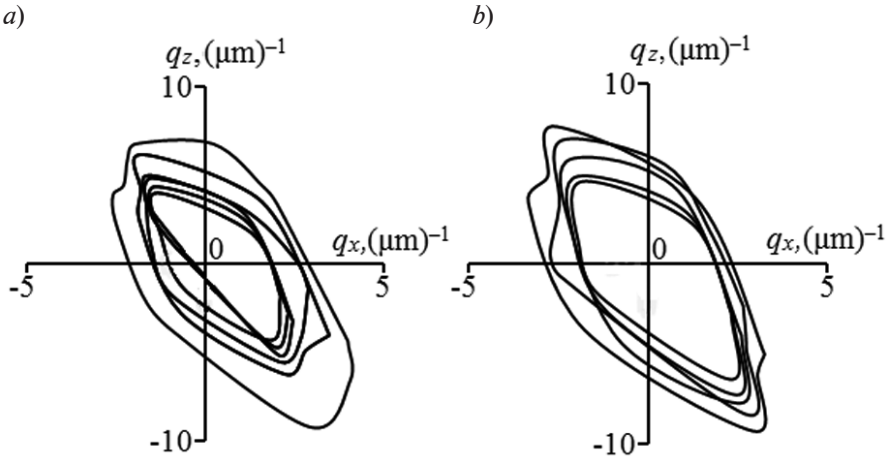

Fig. 2. Equal intensity contours around the (111) reciprocal lattice site for the $Pb_{0.97}Sn_{0.03}Se/PbSe/CaF_2/Si(111)$ structure obtained by TCXRD for the initial (*a*) and the porous (*b*) surface

However, because of the mismatch between the lattice parameters of the substrate and the buffer layer and the parameters of the structure under consideration, caused by the difference in the linear thermal expansion coefficients of the materials of the multilayer system, penetrating dislocations and point defects evolve in the epitaxial film. In addition, the substrate initially had a small lattice deviation from the surface, amounting to approximately 1 – 2 degrees. This led to a slight tilt of the lattice and the grown film.

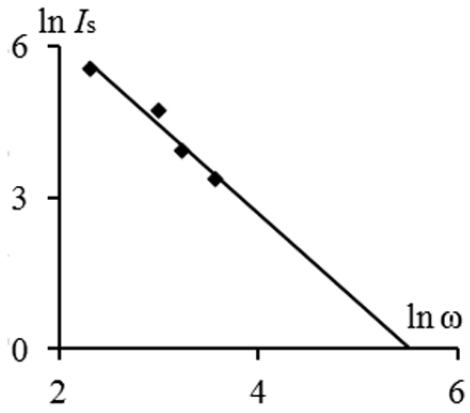

Fig. 3. Linear anamorphosis of the angular dependence of the diffuse scattering peak intensity for the initial $Pb_{0.97}Sn_{0.03}Se/PbSe/CaF_2/Si(111)$ system; the dependence was obtained by the TCXRD method; ω is the angle of rotation of the sample (see Fig. 1, *a*)

Fig. 3 shows the dependence of the diffuse scattering intensity I_s on the TCXRD curves on the sample rotation angle ω (on a double logarithmic scale). It can be seen that the intensity decreases by the ω–*b* law. The parameter *b* was sought by determining the tilt of the curve

$$\ln I_s = f(\ln\omega);$$

it was found to be equal to 1.8.

This value of the parameter indicates that X-ray radiation is scattered mainly by dislocations [8]. The physical nature and the role of dislocations in such systems (lead chalcogenide films on a silicon substrate) are described in detail in [10].

The contours around the (111) reciprocal lattice site are shaped as a tilted oval (see Fig. 2) with indented edges, which corresponds to diffuse scattering by small defects of trigonal symmetry [11]. The shape of the contours becomes more characteristic for diffuse scattering on small defects after anodizing. Pores are typically the main defects formed during anodizing; for this reason, it seems logical to assume that the diffraction pattern in porous $Pb_{0.97}Sn_{0.03}Se$ films is primarily governed by X-ray scattering by pores.

SEM micrographs images of porous film cleavage are shown in Fig. 4. The surfaces of the films exhibit a fairly homogeneous structure (region *1*). After the electrochemical etching process, a porous layer with a thickness of

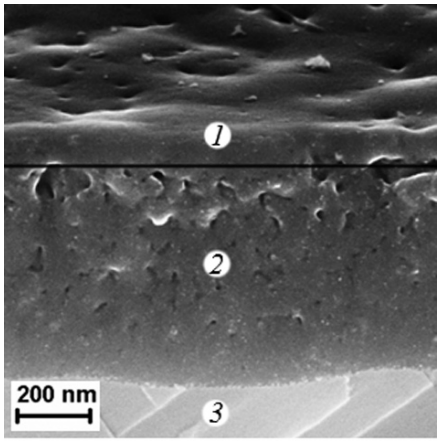

Fig. 4. Micrographs of cleavage of porous lead selenide – tin selenide film; regions of reprecipitated selenium (*1*), the porous structure (*2*), and the unchanged region (*3*) are shown

about 700 nm (region *2*) was formed, and the surface of the sample gained a complex morphology. Notably, a near-surface layer about 50 nm thick (region *1* of the cleavage) had no pronounced pores and was, apparently, a layer of precipitated selenium-based products of electrochemical reactions. This is confirmed by backscattering of electrons at a voltage of 10 kV [7]. An estimate of the geometric porosity (the ratio of the pore area to the total area) over a series of cleavage images showed that the porosity was non-uniform in thickness and varied from 37 % in the upper part to 18 % in the lower part of the porous $Pb_{0.97}Sn_{0.03}Se$ layer under consideration.

Electrochemical anodizing in $Pb_{0.97}Sn_{0.03}Se$ crystals generated pores shaped as parallelepipeds with blurred boundaries [7]. The average pore dimensions along the surface (l_x) and perpendicular to it (l_z) can be estimated from the half-width of the diffuse scattering peaks obtained by rotating the sample crystal at a fixed angular position of the crystal analyzer (ω scan) and (θ/2θ) scans (Fig. 5):

$$l_x \approx \lambda / (2\Delta\theta \cdot \sin\theta_B), \quad (3)$$

$$l_z \approx \lambda / (2\Delta\theta_z \cdot \cos\theta_B), \quad (4)$$

where $\Delta\theta$, $\Delta\theta_z$ are the widths of the diffuse scattering peak on the TCXRD curves taken in the ω and (θ/2θ) scanning modes, respectively (the rotation step of the analyzer is twice as large as that of the sample in the latter of these modes).

The pores are not actually parallelepiped-shaped vertical cavities; they have kinks and are tilted at an angle to the surface of the film [7], which leads to a decrease in average pore sizes over depth. The average angle ξ of pore tilt to the normal of the sample surface can be estimated from the angular position of the diffuse peak on the X-ray patterns taken while rotating the sample crystal at a fixed angular position of the analyzer crystal (see Fig. 5):

$$\mathrm{tg}\xi = q_{x0} / q_{z0}, \quad (5)$$

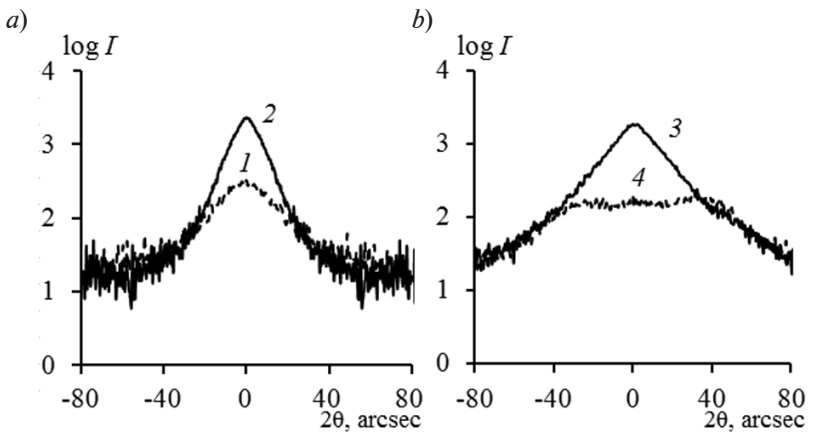

Fig. 5. Diffuse scattering intensities (TCXRD curves) recorded for porous lead selenide – tin selenide in the (θ/2θ) (*a*) and ω (*b*) scanning modes;
curves *1* and *2* were obtained for the initial and the porous surface, respectively; curves *3* and *4* were obtained for the values of the angle ε = 0 and −30 “, respectively

where q_{x0} and q_{z0} are the coordinates of the diffuse peak on the TCXRD cross-sections.

The value of the tilt angle ξ allows to estimate the average values of the transverse (d) and longitudinal (l_l)) pore sizes (perpendicular to and along the surface normal) [8]:

$$d \approx l_x \sin\xi, \quad (6)$$

$$l_l \approx l_z / \sin\xi, \quad (7)$$

where l_x, l_z are the average pore sizes along the surface and over the layer depth.

With a current density of 1 mA/cm^2 and anodizing time of 10 min, the transverse and longitudinal pore projections were 47 and 82 nm, respectively. The average tilt angle of the pores from the normal to the surface was 34.5 degrees. This value is close to the angle of 35 degrees, determined for the propagation of pores in lead telluride films [5] and the corresponding pore formation in the crystallographic direction (110). Interestingly, the longitudinal sizes of the pores turned out to be less than the total thickness of the porous layer, which, apparently, indicates the that through pores broke down into several segments.

Fig. 6 shows the normalized experimental integral curves obtained by X-ray reflectometry before and after electrolytic etching. The depth of X-ray penetration into the sample was minimal and expressed by the extinction length

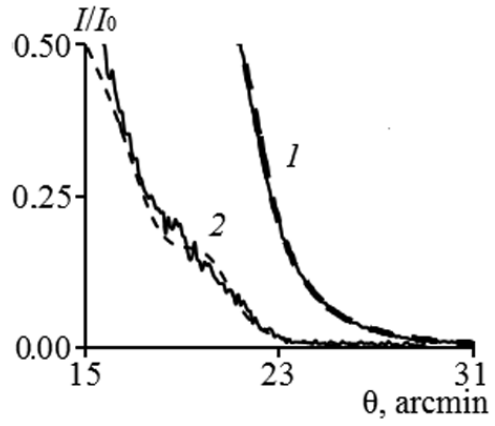

Fig. 6. Experimental (solid lines) and theoretical (dashed lines) curves obtained by X-ray reflectometry for the initial (*1*) and the porous (*2*) surface; $\chi^2 = 0.32$ (*1*) and 2.34 (*2*)

determined by the polarization coefficient χ within the Bragg reflection. The extinction length for a lead selenide single crystal was about 380 nm.

The value of the critical angle on the curves obtained by reflectometry allows to calculate the degree of porosity P for homogeneous systems, that is, the ratio of the pore volume to the sample volume in percent [12, 13]:

$$P = 1 - (\theta_{ca} / \theta_{ci})^2, \quad (8)$$

where θ_{ci} and θ_{ca} are the critical angles on the diffraction curves before and after anodizing, respectively.

The main factors affecting the change in the shape of the diffraction curve are the surface microgeometry and the presence of inhomogeneities in the near-surface region of the sample. The critical angle θ_c was determined from the angular position of the point with an intensity equal to half the height in the region of diminishing intensity. A significant decrease in the θ_c value after anodizing treatment is explained by the increase in the degree of X-ray absorption as a result of the emergence of pores. The degree of porosity was 44 %.

We should note that the extinction length was almost half the thickness of the anodized region (700 nm judging by the image of the cleavage, see Fig. 4) and the degree of porosity was calculated only for the upper region of the porous sample. An additional porous layer of selenium was located on the surface of the porous $Pb_{0.97}Sn_{0.03}Se$ layer in the case under consideration.

Importantly, the critical angles used to determine the porosity depend on the polarization coefficient of the substance, while a part of the near-surface layer about 50 nm thick (1/6th – 1/7th part of the surface) was made up of deposited reaction products. For comparison, the critical angle for a perfect selenium single crystal (0.281°) was less than that for a lead selenide crystal (0.367°). Since the thickness of the selenium layer was 14–17 % of the region under consideration, it is obvious that the influence of this layer on the X-ray reflectometry curves cannot be neglected. As a result, the porosity values in lead-tin selenide, obtained by formula (8), turned out to be overestimated compared to the geometric porosity

value in the upper region of the porous layer. For this reason, the next stage of the study involved the analysis of X-ray reflectometry data for a porous system within the framework of a two-layer model.

A theoretical plot is usually constructed from X-ray reflectometry data to determine the structural parameters of the surface under consideration (see the dashed curves in Fig. 6), achieving a high degree of convergence with the experimental reflectometry curve [14, 15]. An analysis scheme with Parratt's recursion relations for calculating the R_n amplitude of mirror reflection of X-rays from n layers of a given structure is used to construct the theoretical curve [15]:

$$R_n = \frac{r_n + R_{n-1}\exp(2\pi D_n k_n / \lambda)}{1 + r_n R_{n-1}\exp(2\pi D_n k_n / \lambda)}, \quad (9)$$

$$k_n = \sin^2\theta + \chi_n, \quad (10)$$

where θ is the incidence angle of X-rays; χ_n is the polarizability of the material of the nth layer (in the first approximation it is proportional to the electron density in this material); D_n is the thickness of the layer.

The amplitudes r_n of reflection from the boundary of each individual layer are determined by the Fresnel coefficients k_n:

$$r_n = \frac{k_{n+1} - k_n}{k_{n+1} + k_n}\exp\left[-0,5\left(\frac{2\pi}{\lambda}k_n\sigma_n\right)^2\right], \quad (11)$$

where σ_n is the roughness of the layer.

The thickness D_n and the roughness σ_n of the layers were fitted in modeling the theoretical reflectometry curve. The parameters of the $Pb_{0.97}Sn_{0.03}Se$ surface, obtained by minimizing the functional χ^2, are shown in the table. For initial films, we have a fairly flat surface with distinctive triangular nanotraces, typically several nanometers high [5]. The calculated density ρ for the initial surface in the model turned out to be slightly less than that of the lead selenide single crystal. After electrochemical etching, the density of lead-tin selenide decreased by 32 %, compared with tabular values for lead selenide (8.3 g/cm^3). The porosity value of 32 %, found from the density change, is in good agreement with the averaged geometric porosity in the upper half of the porous $Pb_{0.97}Sn_{0.03}Se$ layer. A thin surface layer, presumably consisting of selenium, was discovered for anodized films (tabular density values of various modifications of selenium are in the range of 4.3–4.8 g/cm^3) with a thickness of about 45 nm, which corresponds to the estimates acquired by scanning electron microscopy. The σ_2 value for the second layer is the roughness of the boundaries between the layers.

Conclusion

Thus, the methods of reflectometry and high-resolution X-ray diffraction proved to be effective tools for determining the porosity value and the pore parameters of $Pb_{0.97}Sn_{0.03}Se$

Table

Simulation results of $Pb_{0.97}Sn_{0.03}Se$ layers

Surface (convergence χ^2)	D_n, Å		σ_n, Å		ρ_n, g/cm^3	
	$n = 1$	$n = 2$	$n = 1$	$n = 2$	$n = 1$	$n = 2$
Initial (0.32)	–	–	43	–	7.8	–
Porous (2.34)	450	–	350	50	4.4	5.7

Notations: D_n, σ_n, ρ_n are the thickness, the roughness and the density of the n-th layer.

Notes: 1. The porous surface consists of the near-surface layer and the porous layer itself.
2. The scattering of X-rays by the substrate and the initial non-porous layer was not taken into account in the simulations.

films. We have established that a macroporous structure with transverse pore projections of 47 nm and longitudinal pore projections of 82 nm formed under electrochemical treatment in a Tompkins-Johnson electrolyte at a current density of 1 mA/cm^2. We have found the averaged thickness of the near-surface selenium layer to be 45 nm, which had a significant effect on the porosity value determined by reflectometry. A qualitative agreement has been obtained between the results of X-ray and SEM studies. We have demonstrated the possibilities of using high-resolution X-ray methods for nondestructive investigation of the structure of porous materials.

Acknowledgment

The authors are grateful to H. Zogg (ETH Zurich) for providing the PbSnSe/PbSe/CaF_2/Si(111) films for the studies, and to E.Yu. Buchin (deputy director of the Yaroslavl branch of the Ioffe Institute) for assistance in carrying out anodic treatment.

The study was carried out with the partial financial support of RFBR (grant 13-02-00381).

REFERENCES

[1] Properties of porous silicon, Ed. by L. Canham, Malvern, DERA, 1997.

[2] **A. Cojocaru, M. Leisner, J. Carstensen, H. Föll,** Comparison of currentline pore growth in *n*-type InP and in *n*-type Si, Phys. Stat. Sol. (c). 8 (6) (2011) 1779–1782.

[3] **I.M. Tiginyanu, E. Monaico, V.V. Ursaki, et al.,** Fabrication and photoluminescence properties of porous CdSe, Appl. Phys. Lett. 86 (6) (2005) 063115.

[4] **S.P. Zimin, E.A. Bogoyavlenskaya, E.Yu. Buchin, et al.,** Formation of porous nanostructured lead telluride films by anodic electrochemical etching method, Semicond. Sci. Technol. 24 (10) (2009) 105008(1)–105008(6).

[5] **S.P. Zimin, V.M. Vasin, E.S. Gorlachev, et al.,** Fabrication and study of porous PbTe layers on silicon substrates, Phys. Stat. Sol. (c). 8 (6) (2011) 1801–1804.

[6] **S.P. Zimin, V.M. Vasin, E.S. Gorlachev, et al.,** Investigations of PbSe porous layers by scanning electron microscopy, Phys. Stat. Sol. (c). 8 (6) (2011) 1918–1922.

[7] **S.P. Zimin, E.S. Gorlachev, F.O. Skok, V.V. Naumov,** Investigations of the pore formation in the lead selenide films using glacial acetic acid- and nitric acid-based electrolyte, Nanoscale Research Letters. 7 (1) (2012) 338.

[8] **V.A. Bushuyev, A.P. Petrakov,** Influence of laser annealing on the structure of the surface layers of ion-implanted silicon by X-ray diffractometry, Physics of the Solid State. 35 (2) (1993) 355–364.

[9] **A.A. Lomov, D.Yu. Prokhorov, R.M. Imamov, et al.,** Characterization of porous InP (001) layers by triple-crystal X-ray diffractometry, Crystallography Reports. 51 (5) (2006) 754–760.

[10] **H. Zogg, C. Maissen, S. Blunier, et al.,** Thermal-mismatch strain relaxation mechanisms in heteroepitaxial lead chalcogenide layers on Si substrates, Semicond. Sci. and Technol. 8(1S) (1993) S337–S341.

[11] **M.A. Krivoglaz,** Difraktsiya rentgenovskikh luchey i neytronov v neidealnykh kristallakh [Diffraction of X-rays and neutrons in imperfect crystals], Kiev, Naukova Dumka, 1983.

[12] **A.P. Petrakov,** Issledovaniye pripoverkhnostnykh sloyev veshchestv rentgenovskimi metodami difraktsii, reflektometrii i fazovogo kontrasta [Studies of near-surface substance layers by X-ray diffraction, reflectometry and phase contrast techniques], Syktyvkar, Izd-vo Syktyvkarskogo un-ta, 2007.

[13] **A.P. Petrakov, D.V. Sadovnikov,** Rentgenovskaya reflektometriya poverkhnostey monokristallov, nanokompozitnykh i okisnykh plenok [X-ray reflectometry of monocrystalline surfaces, nanocomposite and oxide films], Vestnik Komi NTs UrO RAN. (9) (2006) 7–9.

[14] **S.N. Yakunin, E.M. Pashaev, A.A. Zaytsev, et al.,** $Si/Si_{1-x}Ge_x$ superlattice structure from X-ray-scattering data, Russian Microelectronics. 34 (4) (2005) 242–251.

[15] **M.A. Chuev, I.A. Subbotin, E.M. Pashaev, et al.,** Phase relations in analysis of glancing incidence X-ray rocking curves from superlattices, JETP Letters. 85 (1) (2007) 17–22.

Received 01.11.2017, accepted 21.11.2017.

THE AUTHORS

MAMONTOV Alexander I.
Vyatka State Humanities University
26 Krasnoarmeyskaya St., Kirov, Kirov region, Volga Federal district, 610002, Russian Federation.
snowchek@mail.ru

PETRAKOV Anatoliy P.
Syktyvkar State University Named after Pitirim Sorokin
55 Oktyabrskiy Ave., Syktyvkar, Republic of Komi, 167001, Russian Federation.
petrakov@syktsu.ru

ZIMIN Sergey P.
P.G. Demidof Yaroslavl State University
14 Sovetskaya St., Yaroslavl, 150000, Russian Federation.
zimin@uniyar.ac.ru